SCIENTIFIC REP🞿RTS

OPEN

The decisive role of free water in determining homogenous ice nucleation behavior of aqueous solutions

Qiang Wang[1], Lishan Zhao[1,2], Chenxi Li[1] & Zexian Cao[1]

It is a challenging issue to quantitatively characterize how the solute and pressure affect the homogeneous ice nucleation in a supercooled solution. By measuring the glass transition behavior of solutions, a universal feature of water-content dependence of glass transition temperature is recognized, which can be used to quantify hydration water in solutions. The amount of free water can then be determined for water-rich solutions, whose mass fraction, X_f, is found to serve as a universal relevant parameter for characterizing the homogeneous ice nucleation temperature, the meting temperature of primary ice, and even the water activity of solutions of electrolytes and smaller organic molecules. Moreover, the effects of hydrated solute and pressure on ice nucleation is comparable, and the pressure, when properly scaled, can be incorporated into the universal parameter X_f. These results help establish the decisive role of free water in determining ice nucleation and other relevant properties of aqueous solutions.

The microscopic mechanism of homogenous ice nucleation in pure water and aqueous solutions has been intensively studied over the past few decades. Although no consensus has been reached yet, the development of solute-free water domains of tetrahedrally coordinated structure is still regarded as the decisive stage of ice nucleation in solution[1–5]. Within such nanosized pure-water domains, a metastable intermediate phase, also called precursor of nucleus, emerges initially with local tetragonal symmetry[6,7] and then grows into ice nucleus composed of randomly stacked layers of cubic and hexagonal sequences[7,8]. The presence of this precursory phase effectively reduces the nucleus/liquid interfacial tension, thus facilitates the occurrence of ice nucleation. A decrease in the probability of forming such precursory phase can explain the suppressing effect of solutes on ice nucleation in solutions[5].

On the other hand, the relationship between the macroscopic features of solutions and the homogeneous ice nucleation temperature, T_H, has also been investigated without considering the microscopic structural details of both the solution and ice nucleus therein. A prominent example is the semi-empirical water activity (a_w) approach[9–12]. This thermodynamic approach stresses that T_H is uniquely related to a_w, irrespective of the chemical nature of the solutes. This liquid-only criterion for the onset of freezing and the classical nucleation theory were suggested to be reconciled if the activation energy for water molecules to cross the nucleus/liquid interface is taken as a function of a_w[9]. Later, a physical basis for this approach was proposed: for pure water under pressure $p \leq 1$ kbar, T_H is nearly coincident with the temperature at which the compressibility of water reaches its maximum value, denoted herein as $T(\kappa_{max})$[10]. Different solutions of the same a_w have the same osmotic pressure, therefore, the same $T(\kappa_{max})$ and T_H. When cooled down to $T(\kappa_{max})$, density or hydrogen boning network fluctuations becomes enough for forming critical-sized low density and tetrahedrally coordinated water domains needed by the formation of ice nucleus.

However, up to now, it still lacks a microscopic understanding of the effect of solute on homogeneous ice nucleation, for instance, how to estimate the effect of solute hydration on ice nucleation. Solute hydration plays an important role in determining many basic thermodynamic and kinetic properties of both solute and solvent

[1]Beijing National Laboratory for Condensed Matter Physics, Institute of Physics, Chinese Academy of Sciences, Beijing 100190, China. [2]Department of Physics, University of Science and Technology Beijing, Beijing 100083, China. Correspondence and requests for materials should be addressed to Q.W. (email: qwang@iphy.ac.cn) or Z.C. (email: zxcao@iphy.ac.cn)
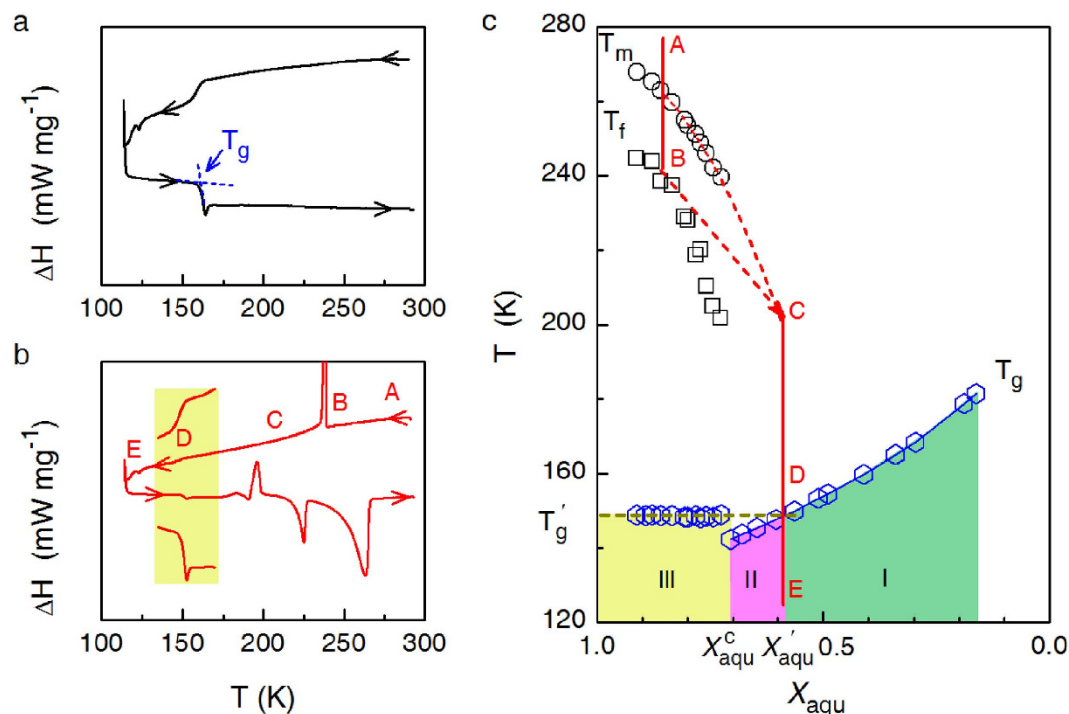
Figure 1. DSC thermograms of aqueous $H_2SO_4 + HNO_3$ solutions with a mass fraction of water of (**a**) $X_{aqu} = 0.39$ and (**b**) $X_{aqu} = 0.85$. $X_{HNO_3} = 0.07$ in both cases. (**c**) State diagram of $H_2SO_4 + HNO_3$ solution. For solutions with $X_{aqu} > X_{aqu}^c$ (zone III), primary ice precipitates first and then the residual freeze-concentrated solution vitrifies, obviously, at an almost constant temperature, termed T_g'. T_m and T_f refer to the melting and freezing points of primary ice precipitated within zone III. As shown in (**b**) and (**c**), during cooling solution with $X_{aqu} = 0.85$ from temperature point A, precipitation of primary ice begins at temperature point B and terminates at temperature point C. Below C, water content in freeze-concentrated solutions keeps nearly constant, which is equal to X_{aqu}'.

in aqueous solutions. For describing a_w, hydration water was suggested to be removed from solvent in calculating the effective concentration of solute[13–16]. But unsatisfactorily, in so doing the hydration number, n_h, has only been simply adopted as an adjustable parameter without rigorous definition or justification[13,17]. To date, this problem still keeps unresolved because hydration water has been defined differently according to different properties of water involved, and n_h has been measured by various experimental techniques, including X-ray and neutron diffraction[17,18], X-ray adsorption[19], differential scanning calorimetric (DSC) measurement[20], as well as Raman[21], nuclear magnetic relaxation[22], terahertz dielectric relaxation[23], and infrared spectroscopies[23,24]. A strict definition of hydration water from the point of view of suppressing ice nucleation and an accurate quantification of n_h will open a possibility of discussing the effect of solute hydration on T_H and even a_w, respectively, which will also help us microscopically understand the relation between a_w and T_H.

When cooled solutions at moderate rates, water molecules in concentrated solutions can totally vitrify[25–28], and those in water-rich solutions partially crystallize into primary ice and partially vitrify together with the solutes. These vitrified water molecules in low temperature phase of water-rich solutions are herein defined as hydration water. The value of n_h was quantified through comparing the glass transition temperature, T_g, of hydration water with those at which concentrated solutions vitrify totally. Very interestingly, we observed that the mass fraction of free water, X_f, can serve as a universal parameter for describing T_H, T_m, and even a_w of solutions of electrolytes and small organic molecules. This observation verified that the hydration water defined herein is rarely involved in the formation of ice nucleus, and contributes negligibly to a_w, at the same time, stressed the key effect of amount of free water on the formability of ice nucleus and on the thermodynamic property of solutions. Moreover, we observed that, in depressing T_H and T_m, pressure is equivalent to the mass fraction of hydrated solute, and also established the quantitative relationship between them.

Results

Quantification of hydration water. We find that the water content dependence of T_g for aqueous solutions displays a quite universal feature, which in turn can provide a simple and reliable method for quantifying hydration number of solutes. Figure 1a,b show the DSC thermograms for the aqueous $H_2SO_4 + HNO_3$ solutions with a mass fraction of water of $X_{aqu} = 0.39$ and 0.85, respectively. The mass fraction of HNO_3 is fixed at $X_{HNo3} = 0.07$. The concentrated $H_2SO_4 + HNO_3$ solutions such as the one with $X_{aqu} = 0.39$ can totally vitrify. This behavior was observed in solutions with increasing water content up to a critical value of $X_{aqu}^c = 0.69$ (Fig. 1c). For

water-rich solutions with $X_{aqu} > X_{aqu}^c$, as illustrated by the sample with $X_{aqu} = 0.85$ in Fig. 1b, crystallization of primary ice occurs firstly, followed by the vitrification of freeze-concentrated solutions.

Those water molecules in vitrified freeze-concentrated solutions are defined as hydration water herein. The corresponding n_h can be deduced from the concentration of the freeze-concentrated solution. Traditionally, this concentration is determined by the point of intersection of T_g curve of concentrated solutions and the extrapolated T_m curve of ice in water-rich solutions. This method is valid mainly for solutions of larger organic molecules which have narrow temperature and/or concentration gaps between T_g and non-extrapolated T_m curves[20,26]. However, the error from extrapolating T_m curve cannot be neglected for solutions of electrolytes and small organic molecules, which have lager temperature and concentration gaps between T_g and non-extrapolated T_m curves. Moreover, it may be unreasonable to extrapolating T_m curve down to T_g curve. As can be seen from Fig. 1b,c, when cooled $H_2SO_4 + HNO_3$ solution of $X_{aqu} = 0.85$ from temperature A, crystallization of primary ice begins at temperature B and finishes at C. Therefore, the concentration of freeze-concentrated solutions keeps constant when further decreasing temperature below C. This problem has already been noticed[28], however, cannot be resolved mainly due to the difficulty in determining C point.

A comparison between T_g of freeze-concentrated solutions and those at which concentrated solutions totally vitrify can accurately determine the concentration of freeze-concentrated solutions. As shown in Fig. 1c, freeze-concentrated solutions vitrify at a nearly constant temperature, denoted as T_g'. Therefore, the concentration of the freeze-concentrated phases corresponds to that of the solution that totally vitrifies at $T_g = T_g'$ determined on the monotonous part of the T_g versus X_{aqu} curve. The determined concentration is denoted as X_{aqu}', at which solution can also be written as $M \cdot n_h H_2O$, here M stands for the solute. With the known X_{aqu}' and X_{aqu}^c, the solutions for a given solute can be categorized into three distinct zones with regard to different vitrification and crystallization behaviors of water (Fig. 1c). For solutions in zone I there is less water to complete the hydration; while solutions in zone III are water-rich, wherein ice precipitation occurs spontaneously in the cooling process. For solutions falling in zone II with $X_{aqu}^c > X_{aqu} > X_{aqu}'$, water can totally vitrify when cooled at moderate rates, however, crystallization of water can still be observed on the reheating process or after performing long-time holding treatment at temperatures above T_g[29]. These recrystallized water molecules are normally named the freezable bound water.

The water-content dependence of T_g depicted in Fig. 1c was also measured in solutions of electrolytes such as LiCl, $CaCl_2$, $Ca(NO_3)_2$, $MnCl_2$, $Mn(NO_3)_2$, $MgCl_2$, $Mg(NO_3)_2$, $Mg(CH_3COO)_2$, $ZnCl_2$, $FeCl_3$, $Fe(NO_3)_3$, $CrCl_3$, $Cr(NO_3)_3$, $AlCl_3$, HNO_3-H_2SO_4, and of simple organic molecules such as glycerol, ethylene glycol (EG), polyethylene glycol (PEG) 300, dimethyl sulfoxide (DMSO), and 1,2,4-butanetriol; and some mixtures such as those of $MgCl_2 + ZnCl_2$, $ZnCl_2 + $ glycerol (see Supplementary Figs. 1–10). Experimental results show that the feature of X_{aqu}-dependent T_g illustrated in Fig. 1c is quite universal at least to the systems investigated and cited in this work. The obtained X_{aqu}' and n_h for the measured solutes are listed in Supplementary Table I.

Mass fraction of free water as pertinent parameter. For dilute solutions in zones II & III with a $X_{aqu} > X_{aqu}'$, which containing more water than hydration, the mass fraction of free water, X_f, can be calculated without any assumption. Briefly, for $M \cdot n H_2O$, X_f is defined by

$$X_f = (n - n_h) \times 18/(n \times 18 + M_s), \tag{1}$$

where M_s is the molar weight of the solute. For any aqueous solutions specified by a $X_{aqu} > X_{aqu}'$, X_f can be directly calculated from

$$X_f = \left[X_{aqu} - X_{aqu}'\right]/\left[1 - X_{aqu}'\right]. \tag{2}$$

Remarkably, the original scattering T_H and T_m data when plotted against X_{aqu} (Fig. 2a) merge into two quite compact curves when plotted as a function of X_f (Fig. 2b), which can be well fitted by the functions $T_H = 247.66 - 162.12 \exp(-2.581 X_f)$ and $T_m = 277.21 - 87.87 \exp(-3.044 X_f)$, respectively. In Fig. 2, all the T_H data are cited from literatures published between 1980 and 2011, which were obtained by measuring emulsified samples with a diameter of $1\sim10\,\mu m$[11,26,30–39]. The T_m data were either extracted from the liquidus lines in the reported phase diagrams[25,26,28,34,39–42] or read from the position of the endothermal peaks on DSC curves measured in the current work. We measured T_m data for solutions of $Mg(CH_3COO)_2$, EG, 1,2,4-butanetriol, glycerol + $ZnCl_2$(1:1), $MgCl_2 + ZnCl_2$(1:1), $MgCl_2 + ZnCl_2$(1:3), and $HNO_3 + H_2SO_4$. Additionally, the observed roughly universal X_f-dependence of T_H and T_m is also valid for electrolytic solutions wherein the freeze-concentrated phase preferably crystallizes instead of undergoing vitrification, such as aqueous solutions of H_2O_2, $(NH_4)_2SO_4$, H_2SO_4, and HNO_3 (see Supplementary Table 1 and the note therein). In this case, free water was still defined as the part of water that crystallizes into primary ice.

Figure 2b indicates that T_H depends solely on X_f and is insensitive to the specific solute-water interaction. This insensitiveness can be attributed to the screening effect of hydration water to the solutes. In other words, the influence of solutes on ice nucleation can be evaluated via the hydration capability of the solute, i.e., n_h, which increases roughly linearly with the Gibbs energies of hydration of cations and molecules (see Supplementary Fig. 11), and increases from 6 for LiCl to about 19 for $AlCl_3$ (Supplementary Table I). As we know, the number of water in the first and second hydration shells of ions is about 6 and 9~20 (depending on the type of cations), respectively[17,18]. Therefore, regarding influence upon ice nucleation occurring in dilute solutions, the solute−water interaction cannot extend beyond the first hydration shell for monovalent electrolytes and simple organic molecules, and cannot extend beyond the second hydration shell for multivalent electrolytes.
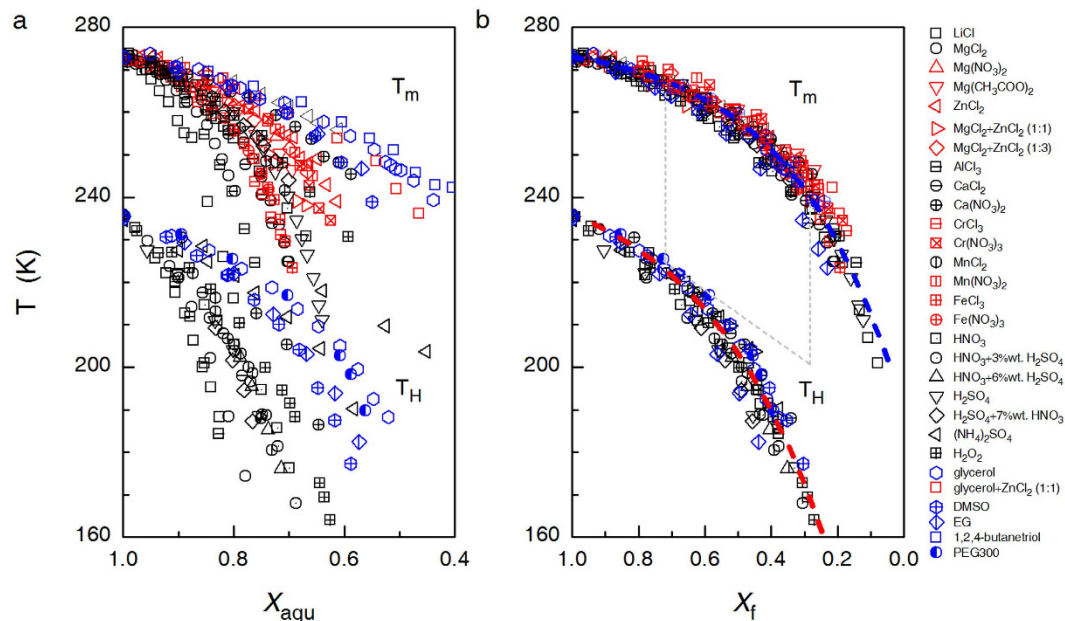
Figure 2. The homogeneous ice nucleation temperature, T_H, and the melting temperature of ice, T_m, as a function of (**a**) mass fraction of water, X_{aqu}, and (**b**) mass fraction of free water, X_f, for various aqueous solutions. For mixed solutions, the composition is specified either with the molar ratio of the solutes or the weight percentage of the minor solute. In (**b**), the dashed lines are added to emphasize the widen gap between T_H and T_m with increasing X_f.

Strictly speaking, n_h can be regarded as a reflection of the ability of solutes to increase the fraction of high-density local heterogeneities in supercooled water. H.E. Stanley *et al.* made a similar suggestion for the effect of pressure on water structure[43]. Moreover, the gap between T_H and T_m curves plotted in Fig. 2b becomes widen with decreasing X_f (or with increasing the mass fraction of hydrated solute $(1 - X_f)$). This behavior is also analogous to the effect of pressure[44]. Therefore, the following text discusses the equivalent relationship between pressure and $(1 - X_f)$ from the point of view of depressing T_H.

The equivalency relation between solute concentration, c, and external pressure, P, with regard to their effect upon reducing T_H has drawn much attention, and such an equivalency relation was first observed in alkali halide solutions[45]. However, no valuable information has ever extracted because the variation of T_H with c is apparently very sensitive to the solute type. Koop *et al.* also analyzed this problem on the basis of the concept of a_w[9]. They found that $T_H(c, P) = T_H(c^{eff}, P = 0)$, where c^{eff} refers to an effective solute concentration, which is defined via the equation $a_w(c, T, P) = a_w(c^{eff}, T, 0)$.

Figure 3a comparatively plots the X_f–dependence of T_H for solutions and P–dependence of T_H for pure water[45]. Obviously, in depressing T_H, P can be linearly scaled against the mass fraction of hydrated solute in the following way:

$$1 - X_f = \alpha_{P \to X_f} P, \tag{3}$$

where P is in MPa, and the coefficient $\alpha_{P \to X_f} = 3.32 \times 10^{-3} \, \mathrm{MPa}^{-1}$. This linear scaling relation in Eq. (3) holds for pressure range $0.1 < P < 200 \, \mathrm{MPa}$, corresponding to $180 \, \mathrm{K} < T_H < 236 \, \mathrm{K}$. This is to say that T_H values are approximately the same for pure water under P and solutions with a mass fraction of free water $X_f = 1 - \alpha_{P \to X_f} P$.

The dominating mechanism for solutes to suppress ice nucleation is to combine with hydration water so as to reduce the amount of free water. We applied this picture to understand the effect of pressure. For a solution of X_f, when further subject to an external pressure of P, an effective mass fraction of free water, X_f^{eff}, can be introduced in analog to the definition for X_f,

$$X_f^{eff} = (n - n_h - n_p) \times 18 / (n \times 18 + M_s), \tag{4}$$

where n_p specifies the effect of the applied pressure on the part of free water denoted by $(n - n_h)$, as if it further reduced the amount of free water as by hydration. By virtue of Eq.(3), it should have

$$n_p / (n - n_h) = \alpha_{P \to X_f} \cdot P. \tag{5}$$

Thus we arrive at the formula.

$$X_f^{eff} = [(n - n_h) \times 18 / (n \times 18 + M_s)] \times [(n - n_h - n_p) / (n - n_h)] = X_f \left(1 - \alpha_{P \to X_f} P\right), \tag{6}$$
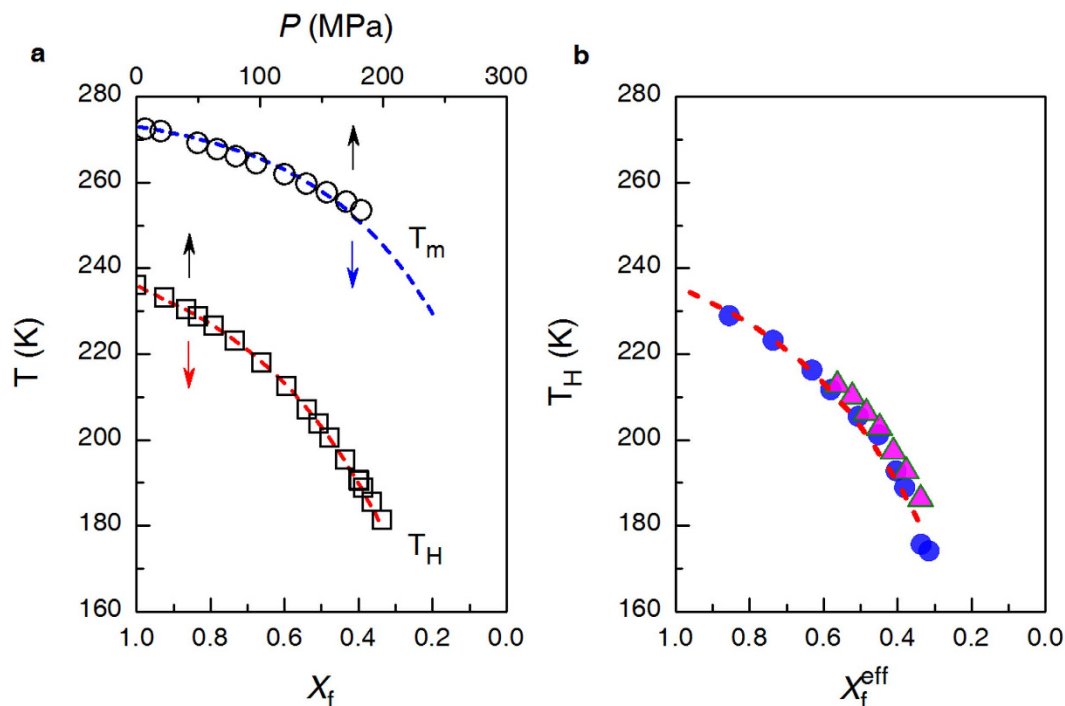
Figure 3. (**a**) The homogeneous ice nucleation temperature, T_H, as a function of pressure, P, for pure water (black square), and of the mass fraction of free water, X_f, fitted for solutions referring to Fig. 2b (red dashed line). For comparison, melting temperature ice, T_m, as a function of pressure for pure water (black circle), and of X_f for solutions (blue dashed line) were also plotted. (**b**) T_H as a function of the effective mass fraction of free water, X_f^{eff}, for pure water under variable pressures and solutions under atmospheric pressure (red dashed line), and for 5.56 mol. kg^{-1} glycerol solutions under pressure up to about 120 MPa (triangle) and for 1.0 mol. kg^{-1} LiCl solution under pressure up to about 190 MPa (circle).

where X_f and $(1 - \alpha_{P \to X_f} \cdot P)$ represent the contributions from solutes and pressure, respectively. Eq.(6) implies that in reducing the amount of free water in a solution, the pressure and the solute work in close collaboration. The hydrated solutes exert influence on the local hydrogen bonding network in water, while, pressure promotes the high-density non-tetrahedral local structure in free water, both lead to the suppression of ice nucleation probability.

Figure 3b shows the X_f^{eff} dependence of T_H for solutions of 1.0 mol. kg^{-1} LiCl[45] and 5.56 mol. kg^{-1} glycerol[46] under pressures up to 200 MPa (for NaCl, see Supplementary Fig. 12). As expected, all the T_H data points fall exclusively onto the same curve referring to that in Fig. 2b. The regular dependence of T_H obtained under various concentrations or pressures on the parameter X_f^{eff} also suggests that the pressure in the given range has almost no bearing on the hydration water of LiCl and glycerol.

Discussion

Interestingly, the T_H data referred to Fig. 2a also merge into a very compact distribution when plotted as a function of a_w[9], which is a good thermodynamic parameter for comprehensively describing the effect of solutes on ice nucleation. a_w and the related osmotic pressure have been widely used to characterize the formability of nano-sized water domains in supercooled solutions[4,10], or the change in entropy and the activation energy required for water molecules to cross the nucleus/liquid interface[9,12]. The application of a_w undoubtedly provides a simplified treatment of the complex interactions among the different components in a solution. However, this simplified treatment also hinders understanding the detailed role of solute in determining ice nucleation, in part because of a lack of general relations between a_w and other features of the solution concerning the solute-water interaction[15].

Figure 4 plots a_w measured at 298 K for various aqueous solutions against X_f. For comparison, Fig. 4 also plots X_f dependence of a_w at T_m for solutions calculated according to the following equation:

$$\Delta G_{exc}(T_m) = RT_m \ln a_w(T_m), \qquad (7)$$

where ΔG_{exc} is the excess Gibbs free energy of supercooled water, which is defined as the excess heat capacity of supercooled bulk water with respect to bulk ice[47], and R is the gas constant. The data points are no more randomly scattered as plotted versus molar fraction of water or even versus molar fraction of free water (Supplementary Figs 13 and 14), rather they fall onto two seemingly distinct branches (Fig. 4). The lower branch includes electrolytic solutions and the solutions of small organic molecules such as 1,2,4-butanetrio, glycerol, and DMSO, all measured at 298 K[13,47–59]. Consequently, the relationship between $a_w(T_m) \sim X_f$ can be deduced by relationship between $a_w(T_m)$ and T_m established according to Eq. (7) and that between T_m and X_f plotted in Fig. 2b. Noticeably, the deduced
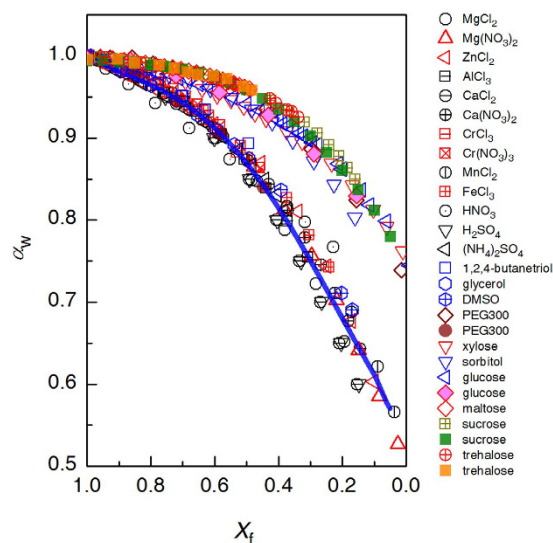
Figure 4. Water activity, a_w, measured at 298 K for various aqueous solutions plotted against X_f (open symbol). Also a_w at T_m for solutions of PEG 300, glucose, sucrose, and trehalose molecules (solid symbol) are included for comparison. The blue solid line results from the calculated $a_w(T_m)$ according to Eq. (7) in conjunction with the $T_m \sim X_f$ relation referred to Fig. 2b.

$a_w(T_m)$ as a function of X_f (blue line) fits well a_w data measured at 298 K for the electrolytic solutions and those of small organic molecules. The a_w data measured at 298 K differ from those measured at the corresponding T_m only negligibly, thus we suggest that n_h is insensitive to temperature.

The quite universal dependences of T_H and $a_w(T_m)$ on X_f, at least for electrolytic solutions, explains the successful application of a_w in describing the effect of solutes on ice nucleation, as a_w indirectly reflects the availability of free water in supercooled solutions.

The above-mentioned fitted T_H versus X_f and T_m versus X_f relations are not valid for solutions of large organic molecules illustrated in Fig. 4, including solutions of xylose, sorbitol, glucose, maltose, sucrose, and trehalose. Obviously these a_w data fall apart from those for electrolytes and small organic molecules, and yet, interestingly, they also roughly merge into one single curve. This difference in a_w versus X_f between electrolytic solutions and those of large organic molecule may lie in the structural heterogeneity in the latter ones. Of the similar X_f levels, the region of free water may be larger due to the aggregation of (unevenly) hydrated large organic molecules, thus manifesting a higher value for a_w and T_H. PEG 300 is an exception, that its data at T_m and at 298 K fall on two branches respectively, i.e., its hydration water number is sensitive to temperature[60].

The $X_f \sim a_w$ relation displaying two distinct branches reminds us that, for the same nominal X_f, it refers to a larger a_w thus a higher T_H for solutions of large organic molecules (data not shown). As T_H depends on the local amount of free water in solution, this clearly results from the structural inhomogeneity in those solutions arising from aggregation of the large organic molecules. Thus one must be cautious in understanding T_H, T_m and other water-related properties for such solutions, since the locally available amount of free water is not necessarily consistent with the nominal concentration of the solution. This case can partially explain the invalidity of colligative property for describing the effect of solutes on T_H and a_w even when hydration is also taken into consideration.

The universal dependence of T_H on X_f, or $T_H(c, P)$ on X_f^{eff}, and even the deviation of $a_w(T_m) \sim X_f$ for electrolytic solutions and solutions of larger organic molecules, lead to recognition of the pivotal role of free water, or the hydration water, in determining the ice nucleation behavior. The solute ions or molecules differ, with regard to suppressing the ice nucleation temperature, in their hydration capability. Ice nucleation in different solutions can thus be understood on the same footing with the concept of hydrated solute or mass fraction of free water. We suggest that hydration of solutes reflect their abilities to increase the fraction of high-density heterogeneities in supercooled water. Different solutions at the same mass fraction of free water have the same temperature dependence of probability of forming critical-sized low-density domain in supercooled free water. However, it still is difficult to estimate the size of the free water domains in solutions from the nominal water content of the solution, as the free water regions are interconnected, and at least in solutions of large organic molecules the distribution of free water may show a severe inhomogeneity. Moreover, a fact remains quite puzzling that why it is mass fraction of free water that universally describe the ice nucleation in solutions.

In summary, by measuring the water-content dependence of glass transition temperature for many different aqueous solutions we recognized that the nearly constant glass transition temperature for the freeze-concentrated phases from the super-cooled water-rich solutions provides a method to quantify the number of hydration water for a given solute. A relevant parameter, the mass fraction of free water, can be well defined and determined. A universal dependence on this parameter was established for the homogeneous ice nucleation temperature, T_H, the melting temperature of primary ice, T_m, and even $a_w(T_m)$. This observation is also valid for water-rich solutions in which the freeze-concentrated phase preferably crystallizes instead of undergoing vitrification. When properly scaled, for suppressing ice nucleation, the effect of pressure can be incorporated into an effective mass

fraction of free water. The one-to-one correspondence between water activity and mass fraction of free water (for electrolytic solutions to the least) explains the validity of water activity in describing the homogeneous ice nucleation behavior in supercooled solutions. It reveals the fact that water activity is essentially a measure of free water.

Methods

Samples. High-purity water was prepared by using a Millipore Milli-Q system. The solutes LiCl (anhydrous, 99.99%), CaCl$_2$ (anhydrous, 99.99%), Ca(NO$_3$)$_2$·4H$_2$O (ACS reagent, 99%), MgCl$_2$ (anhydrous, 99.99%), MnCl$_2$·4H$_2$O (99.99%), ZnCl$_2$ (anhydrous, 99.99%), CrCl$_3$·6H$_2$O (98.0%), AlCl$_3$·6H$_2$O (99%), FeCl$_3$·6H$_2$O (99%), HNO$_3$ (70%, purified by re-distillation to 99.999%), glycerol (99.5%), ethylene glycol (anhydrous, 99.8%), dimethyl sulfoxide(anhydrous, 99.9%), polyethylene glycol 300 (BioUltra) were purchased from Sigma-Aldrich. Other solutes include H$_2$O$_2$ (50 wt.% in H$_2$O, 85 wt.% in H$_2$O, Beijing Chem. Tech. Co.) and H$_2$SO$_4$ (98%, Sinopharm Chemical Reagent).

Thermal measurement. Differential scanning calorimetric measurement on droplets ($\sim$5.0 μL) of aqueous solutions was performed on a calorimeter (PE DSC8000) operating at a cooling/heating rate of 20 K min.$^{-1}$ unless otherwise specified. When cooled down to 110 K, the sample was held at this temperature for 1 min. before the heating procedure began. All of the DSC curves were normalized against sample weight.

References

1. Matsumoto, M., Saito, S. & Ohmine, I. Molecular dynamics simulation of the ice nucleation and growth process leading to water freezing. *Nature* **416,** 409–413 (2002).
2. Moore, E. B. & Molinero, V. Structural transformation in supercooled water controls the crystallization rate of ice. *Nature* **479,** 506–509 (2011).
3. Sellberg, J. A. *et al.* Ultrafast X-ray probing of water structure below the homogeneous ice nucleation temperature. *Nature* **510,** 381–384 (2014).
4. Bullock, G. & Molinero, V. Low-density liquid water is the mother of ice: on the relation between mesostructure, thermodynamics and ice crystallization in solutions. *Faraday Discuss.* **167,** 371–388 (2013).
5. Warkentin, M., Sethna, J. P. & Thorne, R. E. Critical droplet theory explains the glass formability of aqueous solutions. *Phys. Rev. Lett.* **110,** 015703 (2013).
6. Singh, R. S. & Bagchi, B. Correlation between thermodynamic anomalies and pathways of ice nucleation in supercooled water. *J. Chem. Phys.* **140,** 164503 (2014).
7. Russo, J., Romano, F. & Tanaka, H. New metastable form of ice and its role in the homogeneous crystallization of water. *Nat. Mater.* **13,** 733–739 (2014).
8. Malkin, T. L., Murray, B. J., Brukhno, A. V., Anwar, J. & Salzmann, C. G. Structure of ice crystallized from supercooled water. *Proc. Natl. Acad. Sci. USA* **109,** 1041–1045 (2012).
9. Koop, T., Luo, B., Tsias, A. & Peter, T. Water activity as the determinant for homogeneous ice nucleation in aqueous solutions. *Nature* **406,** 611–614 (2000).
10. Baker, M. B. & Baker, M. A new look at homogeneous freezing of water. *Geophys. Res. Lett.* **31,** L19102 (2004).
11. Zobrist, B., Marcolli, C., Peter, T. & Koop, T. Heterogeneous ice nucleation in aqueous solutions: the role of water activity. *J. Phys. Chem. A* **112,** 3965–3975 (2008).
12. Barahona, D. Analysis of the effect of water activity on ice formation using a new thermodynamic framework. *Atmos. Chem. Phys.* **14,** 7665–7680 (2014).
13. Stokes, R. H. & Robinson, R. A. Ionic hydration and activity in electrolyte solutions. *J. Am. Chem. Soc.* **70,** 1870–1878 (1948).
14. Zavitsas, A. A. Properties of water solutions of electrolytes and nonelectrolytes. *J. Phys. Chem. B* **105,** 7805–7817 (2001).
15. Blandamer, M. J., Engberts, J. B., Gleeson, P. T. & Reis, J. C. Activity of water in aqueous systems; a frequently neglected property. *Chem. Soc. Rev.* **34,** 440–458 (2005).
16. Zavitsas, A. A. The Nature of aqueous solutions: Insights into multiple facets of chemistry and biochemistry from freezing-point depressions. *Chem. Eur. J.* **16,** 5942–5960 (2010).
17. Marcus, Y. Ionic-radii in aqueous-solutions. *Chem. Rev.* **88,** 1475–1498 (1988).
18. Ohtaki, H. & Radnai, T. Structure and dynamics of hydrated ions. *Chem. Rev.* **93,** 1157–1204 (1993).
19. Waluyo, I. *et al.* The structure of water in the hydration shell of cations from x-ray Raman and small angle x-ray scattering measurements. *J. Chem. Phys.* **134,** 064513 (2011).
20. Slade, L. & Levine, H. Beyond Water Activity - Recent advances based on an alternative approach to the assessment of food quality and safety. *Crit. Rev. Food Sci.* **30,** 115–360 (1991).
21. Sum, A. K., Burruss, R. C. & Sloan, E. D. Measurement of clathrate hydrates via Raman spectroscopy. *J. Phys. Chem. B* **101,** 7371–7377 (1997).
22. Tait, M. D., Suggett, A., Franks, F., Ablett, S. & Quickenden, P. A. Hydration of monosaccharides: A study by dielectric and nuclear magnetic relaxation. *J. Solution Chem.* **1,** 131–151 (1972).
23. Tielrooij, K. J., Garcia-Araez, N., Bonn, M. & Bakker, H. J. Cooperativity in ion hydration. *Science* **328,** 1006–1009 (2010).
24. Fayer, M. D. *et al.* Water Dynamics in salt solutions studied with ultrafast two-dimensional infrared (2D IR) vibrational echo spectroscopy. *Acc. Chem. Res.* **42,** 1210–1219 (2009).
25. Angell, C. A. Glass-Forming Composition Regions and Glass Transition Temperatures for Aqueous Electrolyte Solutions. *J. Chem. Phys.* **52,** 1058 (1970).
26. Zobrist, B., Marcolli, C., Pedernera, D. A. & Koop, T. Do atmospheric aerosols form glasses? *Atmos. Chem. Phys.* **8,** 5221–5244 (2008).
27. Koop, T., Bookhold, J., Shiraiwa, M. & Poschl, U. Glass transition and phase state of organic compounds: dependency on molecular properties and implications for secondary organic aerosols in the atmosphere. *Phys. Chem. Chem. Phys.* **13,** 19238–19255 (2011).
28. Kobayashi, M. & Tanaka, H. Relationship between the phase diagram, the glass-forming ability, and the fragility of a water/salt mixture. *J. Phys. Chem. B* **115,** 14077–14090 (2011).
29. Zhao, L. S., Cao, Z. X. & Wang, Q. Glass transition of aqueous solutions involving annealing-induced ice recrystallization resolves liquid-liquid transition puzzle of water. *Sci. Rep.* **5,** 15714, doi: 10.1038/srep15714 (2015).
30. Miyata, K., Kanno, H., Tomizawa, K. & Yoshimura, Y. Supercooling of aqueous solutions of alkali chlorides and acetates. *Bull. Chem. Soc. Jpn.* **74,** 1629–1633 (2001).
31. Kumar, A. Homogeneous nucleation temperatures in aqueous mixed salt solutions. *J. Phys. Chem. B* **111,** 10985–10991 (2007).
32. Angell, C. A., Sare, E. J., Donnella, J. & Macfarlane, D. R. Homogeneous nucleation and glass-transition temperatures in solutions of Li salts in D$_2$O and H$_2$O - Doubly unstable glass regions. *J. Phys. Chem.* **85,** 1461–1464 (1981).
33. Bogdan, A., Molina, M. J., Tenhu, H., Mayer, E. & Loerting, T. Formation of mixed-phase particles during the freezing of polar stratospheric ice clouds. *Nat. Chem.* **2,** 197–201 (2010).

34. Bogdan, A. & Molina, M. J. Why does large relative humidity with respect to ice persist in cirrus ice clouds? *J. Phys. Chem. A* **113,** 14123–14130 (2009).
35. Bogdan, A. & Loerting, T. Impact of substrate, aging, and size on the two freezing events of (NH₄)₂SO₄/H₂O droplets. *J. Phys. Chem. C* **115,** 10682–10693 (2011).
36. Bertram, A. K., Koop, T., Molina, L. T. & Molina, M. J. Ice formation in (NH₄)₂SO₄-H₂O particles. *J. Phys. Chem. A* **104,** 584–588 (2000).
37. Oguni, M. & Angell, C. A. Heat-capacities of H₂O + H₂O₂, and H₂O + N₂H₄, binary-solutions - isolation of a singular component for C_p of supercooled water. *J. Chem. Phys.* **73,** 1948–1954 (1980).
38. Miyata, K. & Kanno, H. Supercooling behavior of aqueous solutions of alcohols and saccharides. *J. Mol. Liq.* **119,** 189–193 (2005).
39. Zobrist, B., Weers, U. & Koop, T. Ice nucleation in aqueous solutions of poly[ethylene glycol] with different molar mass. *J. Chem. Phys.* **118,** 10254 (2003).
40. Angell, C. A. Liquid fragility and the glass transition in water and aqueous solutions. *Chem. Rev.* **102,** 2627–2649 (2002).
41. Murata, K. I. & Tanaka, H. Liquid-liquid transition without macroscopic phase separation in a water-glycerol mixture. *Nat. Mater.* **11,** 436–443 (2012).
42. Horsak, I. & Slama, I. Calculation of the phase-diagram for the system water dimethylsulfoxide. *Collect. Czech. Chem. Commun.* **48,** 1936–1943 (1983).
43. Canpolat, M. *et al.* Local structural heterogeneities in liquid water under pressure. *Chem. Phys. Lett.* **294,** 9–12 (1998).
44. Kanno, H., Speedy, R. J. & Angell, C. A. Supercooling of water to −92 °C under pressure. *Science* **189,** 880–881 (1975).
45. Kanno, H. & Angell, C. A. Homogeneous nucleation and glass formation in aqueous alkali-halide solutions at high-pressures. *J. Phys. Chem.* **81,** 2639–2643 (1977).
46. Miyata, K., Hayakawa, S., Kajiwara, K. & Kanno, H. Supercooling and vitrification of aqueous glycerol solutions at normal and high pressures. *Cryobiology* **65,** 113–116 (2012).
47. Johari, G. P., Fleissner, G., Hallbrucker, A. & Mayer, E. Thermodynamic continuity between glassy and normal water. *J. Phys. Chem.* **98,** 4719–4725 (1994).
48. Cohen, M. D., Flagan, R. C. & Seinfeld, J. H. Studies of concentrated electrolyte-solutions using the electrodynamic balance .1. Water activities for single-electrolyte solutions. *J. Phys. Chem.* **91,** 4563–4574 (1987).
49. Robinson, R. A. & Stokes, R. H. Tables of osmotic and activity coefficients of electrolytes in aqueous solution at 25 °C. *Trans. Faraday Society* **45,** 612–624 (1949).
50. Stokes, R. H. & Robinson, R. A. Interactions in aqueous nonelectrolyte solutions .I. Solute-solvent equilibria. *J. Phys. Chem.* **70,** 2126–2130 (1966).
51. Ha, Z. Y. & Chan, C. K. The water activities of MgCl₂, Mg(NO₃)₂, MgSO₄, and their mixtures. *Aerosol Sci. Technol.* **31,** 154–169 (1999).
52. Sadowska, T. & Libus, W. Thermodynamic properties and solution equilibria of aqueous bivalent transition-metal nitrates and magnesium-nitrate. *J. Solution Chem.* **11,** 457–468 (1982).
53. Robinson, R. A. & Stokes, R. H. *Electrolyte Solutions.* (DOVER PUBLICATIONS, INC., 2002).
54. Anstiss, R. G. & Pitzer, K. S. Thermodynamics of very concentrated aqueous-electrolytes-LiCl, ZnCl₂, and ZnCl₂-NaCl at 25 °C. *J. Solution Chem.* **20,** 849–858 (1991).
55. Zeleznik, F. J. Thermodynamic properties of the aqueous sulfuric-acid system to 350 K. *J. Phys. Chem. Ref. Data* **20,** 1157–1200 (1991).
56. Ninni, L., Camargo, M. S. & Meirelles, A. J. A. Water activity in polyol systems. *J. Chem. Eng. Data* **45,** 654–660 (2000).
57. Lam, S. Y. & Benoit, R. L. Some thermodynamic properties of dimethylsulfoxide-water and propylene carbonate-water systems at 25 °C. *Can. J. Chem.-Rev. Can. Chim.* **52,** 718–722 (1974).
58. Ben Gaida, L., Dussap, C. G. & Gros, J. B. Variable hydration of small carbohydrates for predicting equilibrium properties in diluted and concentrated solutions. *Food Chem.* **96,** 387–401 (2006).
59. Miyajima, K., Sawada, M. & Nakagaki, M. Studies on aqueous-solutions of saccharides .2. Viscosity b-coefficients, apparent molar volumes, and activity-coefficients of d-glucose, maltose, and maltotriose in aqueous-solutions. *Bull. Chem. Soc. Jpn.* **56,** 1954–1957 (1983).
60. Koop, T. Homogeneous ice nucleation in water and aqueous solutions. *Z. Phys. Chem.* **218,** 1231–1258 (2004).

Acknowledgements

Author Contributions

Q.W. initiated the research, L.Z., C. L. and Q.W. performed the measurement, Q.W. and Z.C. interpreted the result, Q.W. and Z.C. compiled the manuscript. All authors have given approval to the final version of the manuscript.

Additional Information

Supplementary information accompanies this paper at http://www.nature.com/srep

Competing financial interests: The authors declare no competing financial interests.

How to cite this article: Wang, Q. *et al.* The decisive role of free water in determining homogenous ice nucleation behavior of aqueous solutions. *Sci. Rep.* **6,** 26831; doi: 10.1038/srep26831 (2016).